pyramid reduction,
image analysis,
split and merge method,
aorta structure visualization

Ewelina SOBOTNICKA[1], Aleksander SOBOTNICKI[1], Janusz JEŻEWSKI[1]

GAUSSIAN PYRAMID REDUCTION METHOD FOR THE EXTRACTION OF PATHOLOGICAL STRUCTURES OF THE AORTA

An analysis of the biomedical image in one scale may result in the loss of information contained in the image during an analysis in a different scale. This issue can be solved by an analysis performed simultaneously in all scales, which can be done through the application of the pyramid reduction method. The pyramid makes it possible to obtain images at various levels of detail, including significant information. The paper discusses the method of processing biomedical images of the aorta with the use of the pyramid reduction method, as well as the way in which the results can be used in the segmentation process. The Gaussian pyramid reduction method was used for pyramid representation, whereas the segmentation process was performed with the split and merge method.

1. INTRODUCTION

The paper considers the method of biomedical image processing with the use of the Gaussian pyramid reduction method. Image pyramids make up a hierarchical structure whose size and geometrical resolution can decrease or increase. The pyramid may be interpreted as a multi-level smoothing filter, where superfluous information contained in the image is gradually eliminated, while the most significant objects and structures at the highest level of the pyramid are retained [1], [6], [7]. Pyramid images are reduced versions of the previous image and are successively generated from the original image at the lowest level of the pyramid. At subsequent levels, resolution is reduced two times by eliminating every other row and column of pixels. Correlation begins at the lowest level of the pyramid, next it passes to higher levels until it reaches the highest one. As a result, reduced images are produced. Correlation occurs in accordance with the ”from general to detail” rule [3], [4]. The application of the image pyramid makes it possible to improve the readability of the image and identify subtle details that are difficult to see.
Often, while medical images are being processed, an issue occurs with the search of specific structures or objects that can be found in them. The searched object may expand outside the boundaries of the blocks that the image is divided into. Hence, it is unlikely to be detected although it is located in the image. The analyzed structure may be located in a different spot on the next layer of the image, so it will not be detected, either. While processing specific

[1]Institute of Medical Technology and Equipment, 118 Roosevelt St., 41-800 Zabrze, Poland, {esobotnicka, aleksander.sobotnicki, jezewski}@itam.zabrze.pl

biomedical images, attention should be paid to a proper search for specific regions and proper outlines of the contours. Moreover, the division of the image into smaller elements improves the quality of the search, therefore a decision was made to use the Gaussian pyramid reduction method as one of the tools for preliminary processing and indication of specific structures found in biomedical images.

2. METHODOLOGY

The image analysis process was divided into several stages. At the first stage, a database of aorta images was created. At the second stage, the Gaussian pyramid reduction method was applied to reduce the scale of these images. At the final stage of the work, the images obtained in the pyramid method were used for segmentation to isolate the aorta structure. As a reference shape for segmentation, the authors used the aorta mask created on the basis of the contours made by the authors following a visual examination. In order to verify the correctness of segmentation, a basic statistical analysis was carried out, consisting in the calculation of the Dice coefficient. The stages of the aorta image analysis process were presented in the diagram, Fig. 1.

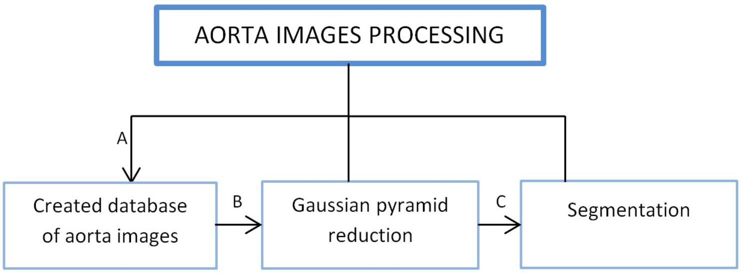

Fig. 1. Stages of aorta images processing.

The experiment was chiefly aimed at isolating the structure of the aorta from the analyzed images, with a clear indication of the contours. To this end, the image had to be prepared and then properly processed. At the initial stage, the images were reduced in scale, and next segmented with the split and merge method. Image processing was carried out in the MATLAB environment with the use of algorithms devised by the authors of this paper.

2.1. Aorta image database

The database containing images featuring the structure of the aorta was created to standardize the set of images from various examinations of various patients, but showing the same structure. The material that the authors had at their disposal consisted of 240 images in the DICOM format, size of 512×512 pixels and depth of 8 bits. The analysis involved images from 5 patients diagnosed with Computed Tomography Angiography (CTA) in various projections: in the CTA projection with contrast of 30%, 60% and 70%, and in the chest projection, Fig. 2. The data used for the analysis consisted of 20 up−to−date CT images, four images from each of the five patients.

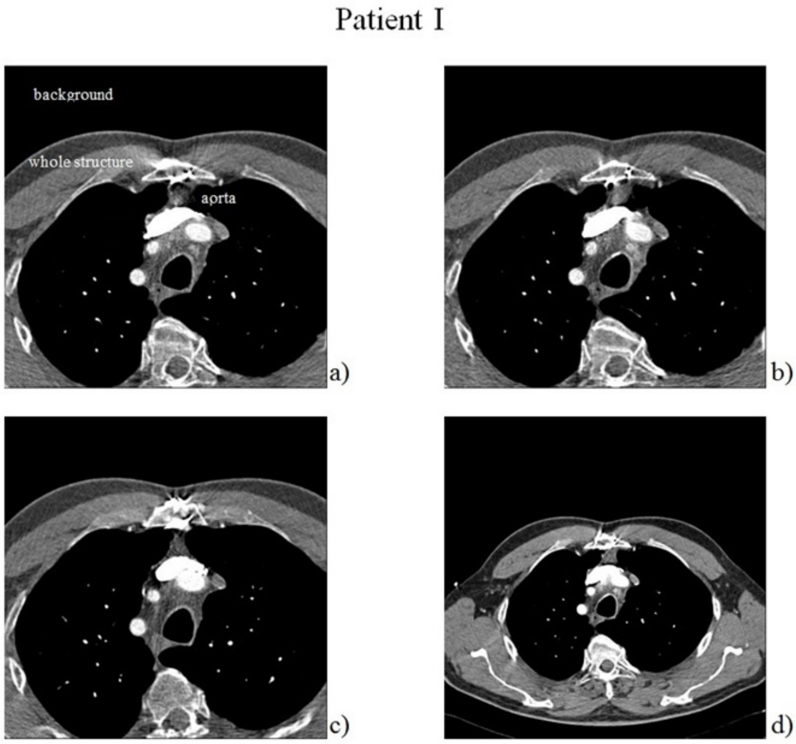

Fig. 2. Examples of original images from a CT examination of patient no. 1. Next, projections were presented with the use of a) contrast 0.6 60%, b) 0.6 30%, c) 0.6 70%. d) view of the chest projection.

2.2. Gaussian spatial pyramid representation

The pyramid method, deployed in the paper, consists in the reduction of the scale of the image. Decomposition leads to data compression, which has a positive impact on the efficiency of the processing algorithm with no significant degradation of the medical image. In [6], the authors proposed the Gaussian pyramid reduction method and divided the image into smaller and smaller regions, at the same time merging the histograms of properties found within each local region. In order to reduce the scale of the images, the authors of the aforementioned paper also deployed the histogram merging method together with the Gaussian sampling method with reference to specific medical images depicting the aorta, which is a new approach in processing. The Gaussian pyramid reduction method is based on multiple division of the region of interest, located in the image, or on the division of the entire image [1]. The area of the image is divided in cycles into more and more blocks. The number of blocks depends on the number of levels of the pyramid, defined beforehand. During division, histograms are created for each block. The histograms correspond to images at subsequent steps of the pyramid. The histogram of the image that was not divided into blocks is found at level zero. The first level represents an image divided into halves alongside each axis. Four blocks are obtained as a result of the division, for which histograms are calculated. At the next levels of the pyramid, the obtained blocks are divided into subsequent quarters. After the image is divided into as many levels as the pyramid consists of, the obtained histograms are merged into one vector, Fig. 3. The process of merging histograms is described by the dependence [3], [4]:

$$H = [\beta_0 * h_0, \beta_1 * h_{1.0}, \beta_1 * h_{1.1}, \beta_1 * h_{1.2}, \beta_1 * h_{1.3}, \beta_2 * h_{2.0.0}, ..., \beta_n * h_n, ...], \tag{1}$$

$$\Sigma_{i=0}^{n} \beta_i = 1, \tag{2}$$

$$\beta_i = \frac{1}{2^{L-i}} \qquad \text{for } i \geqslant 1, \tag{3}$$

$$\beta_i = \frac{1}{2^{L-i}} \qquad \text{for } i = 0, \tag{4}$$

where:
β_i - the weight of the histogram at the i-th level of the pyramid,
$h_{i.j.k}$ - the histogram for subsequent quarters of the i-th level of the pyramid,
L - the number of the categories of objects to be identified.

A graphic presentation of the Gaussian pyramid reduction method is shown in Fig. 3. The image at the zero level includes objects belonging to three categories. The objects are represented by the following symbols: stars, rhombi and squares. Images represented by the first (denoted as 1) and second (denoted as 2) levels were divided. Next, histograms of objects – symbols [6] were placed for images at various resolution levels.

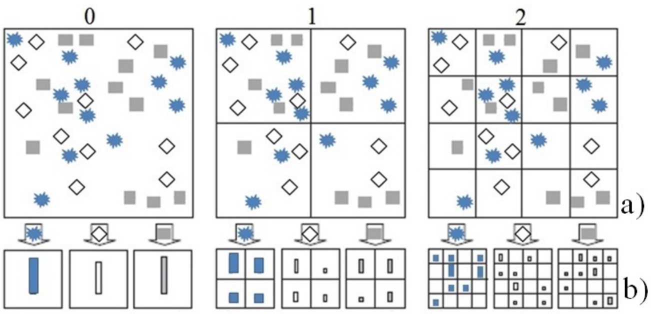

Fig. 3. a) An instance of the Gaussian pyramid reduction at its subsequent levels and b) histograms of objects located in the images, from the left – an image that was not divided at the zero level, subsequent images divided at the first and second levels.

An image divided into four parts and containing four histograms is obtained at the first level of the pyramid. As many as 16 histograms are obtained at the second level of the pyramid. The weight of each histogram at a specific division level should be calculated. In the case under scrutiny, referring to aorta images, the weight of the histogram at the zero level for the identification of three categories of objects (background, the whole anatomical structure and aorta) amounts to:$\beta_0 = 1/2^{3-1} = 1/4$. At the first level it equals $\beta_1 = 1/4$, while at the second level it is equal to $\beta_2 = 1/2$.

2.2.1. THE GAUSSIAN REDUCTION METHOD

During scale reduction, the image at the lowest level of the Gaussian pyramid was its zero level. Next, images at subsequent levels were obtained as a result of reduction of images at previous levels. The process of averaging subsequent levels of the pyramid was performed with the use of the reduction function, described by dependence [3], [4]:

$$im_k = reduce(im_{k-1}), \tag{5}$$

where reduce for levels $0 < l < N$; and nodes $i, j, 0 \leqslant i < K_l; 0 \leqslant j < W_l$.

$$im_l(i,j) = \sum_{m}^{2} = -2\sum_{n}^{2} = -2w(m,n) \times im_{l-1}(2i+m, 2j+n), \tag{6}$$

and where N refers to the number of levels in the pyramid, while K_l and W_l are the dimensions of the l-th level. The values of nodes at the zero level are the gray level of a corresponding image pixel. The values of nodes at a high level are the weighted average of node values at the next lower level. A higher level (low resolution) in a Gaussian pyramid was formed by removing consecutive rows and columns in a lower level (higher resolution) image. Then each pixel at a higher level was formed by the contribution from 5 pixels in the underlying level with Gaussian weights. By doing so, a $K \times W$ image becomes $K/2 \times W/2$ image. So, the area is reduced to one-fourth of original area. The same pattern continues as we go upward in the pyramid. Similarly, while expanding, the area becomes increases 4 times at each level [1]. In our application, Gaussian pyramid reduction was performed by using the $Pyram_{red}$ function which means: $Im = Pyram_{red(Im0)}$. If $Im0$ is a K by W then the size of Im is $(K/2)$ by $(W/2)$. The reduction operation was carried out by convolving the image with a Gaussian low-pass filter. The filter mask was designed in such a way that the center pixel gets more weight than the neighboring ones, and the remaining terms were chosen so that their sum is 1. As a result of scale reduction, three smaller images were obtained, in which specific regions of interest could be isolated in a clear manner, and which provided a basis for segmentation; Fig. 4, Fig. 5.

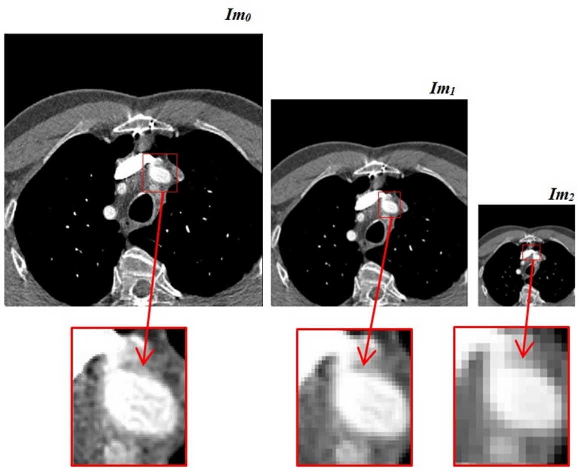

Fig. 4. The Gaussian pyramid reduction method, reduced images from the first patient in projection, contrast 0.6 30%. The obtained pyramid images: $Im0$ – image at the zero level, $Im1$ – image at the first level, $Im2$ – image at the second level of the reduction pyramid.

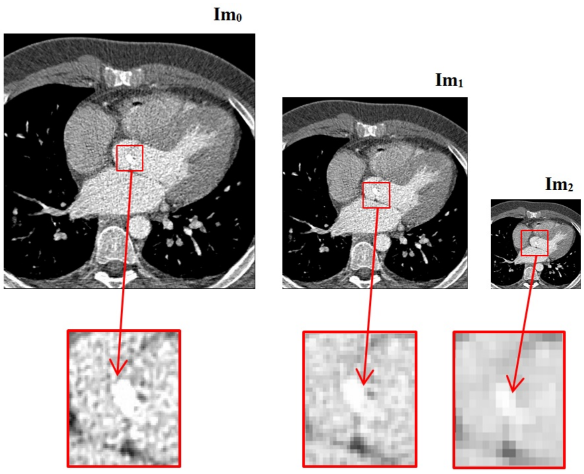

Fig. 5. The Gaussian pyramid reduction method, reduced images from the fifth patient in projection, contrast 0.6 70%. The obtained images: $Im0$ – image at the zero level, $Im1$ –image at the first level, $Im2$ – image at the second level of the reduction pyramid.

2.3. Segmentation of reduced aorta images

In their previous papers, the authors described in detail various segmentation methods and their application in medical images depicting various anatomical structures [9], [12], [13]. The results obtained during research confirm the fact that the split and merge method [13] is best suited for the segmentation of aorta images, hence it was modified, and the Gaussian pyramid reduction, i.e. the preliminary processing element, was added. The segmentation method consists of two phases: splitting and merging. During the splitting phase, the image is divided into blocks by means of the quadtree method. The splitting phase takes place after the splitting criterion is met. If the difference between the maximum and minimum intensity within the analysed block exceeds the threshold intensity value, then the block is subdivided into four smaller blocks; if not, the division of this part of the image ends at this point [2], [11]. Blocks are merged iteratively after the merging criterion for two blocks is fulfilled, i.e. the difference between average intensities is not larger than the merging parameter analysed in the range <0,1>. The value of the splitting and merging parameter was set at 0.5. The values of the analyzed parameters were selected experimentally based on literature data specifying their ranges for the best segmented images [5], [8], [13]. After all blocks and their neighbors are analysed, the current number of blocks is defined. If the number of blocks is equal to that in the previous iteration, then segmentation is regarded as completed.

3. RESULTS

During the experiment, the scale of aorta images was reduced with the pyramid method. The level of the pyramid (decomposition level) to which the images were reduced, was set at 2. 20 different aorta images were used for the analysis. The results obtained during the preliminary analysis are presented as examples in Figs 4 and 5. Images at subsequent decomposition levels ($Im0$, $Im1$, $Im2$) are increasingly sharp, but the contours of the objects are more and more blurred, hence the experiment was ended at the second level of decomposition as this is where the most valuable information is provided. Increased density of image samples, causing data compression, was noticed at subsequent reduction stages. However, the amount of details in the image, irrelevant to the analysis, was reduced. The reduced image contains petty elements that are hardly visible with the ”naked eye”, but this is sufficient for the purposes of segmentation. Owing to preliminary processing consisting in the reduction of scale, it is possible to isolate the aorta structure from the image in the segmentation process, without pixel overflow. During segmentation, at the division stage for the original image $Im0$, an image consisting of 260 blocks was obtained for set values of threshold intensity and the division parameter equal to 0.5. In the course of segmentation of subsequent images, the number of the blocks was reduced and amounted to 242 for image $Im1$ and 147 for $Im2$, respectively. The decreasing number of the blocks at the division stage resulted in a reduced number of iterations performed during the merging phase. Fig. 6 a) demonstrates symmetry and contours of the structures in the image (black arrows point to regions subject to analysis). The higher the level of the pyramid, the more segmented regions there are. The lower the level of the pyramid at which the image is analyzed, the more precise is the segmentation, and the region in which a specific structure occurs is more visibly outlined,Fig. 6 b).

In order to check the correctness and usefulness of the pyramid reduction method, the Dice coefficient was calculated for use in segmentation algorithms, with formula (7) [13]:

$$Dic = \frac{2|im2 \bigcap im1|}{|im2| + |im1|}, \tag{7}$$

where:
$im1$ - binary mask of the original structure,
$im2$ - binary mask of the final result of segmentation,
$im2 \bigcap im1$ - the number of pixels describing the analyzed structure in both compared masks.

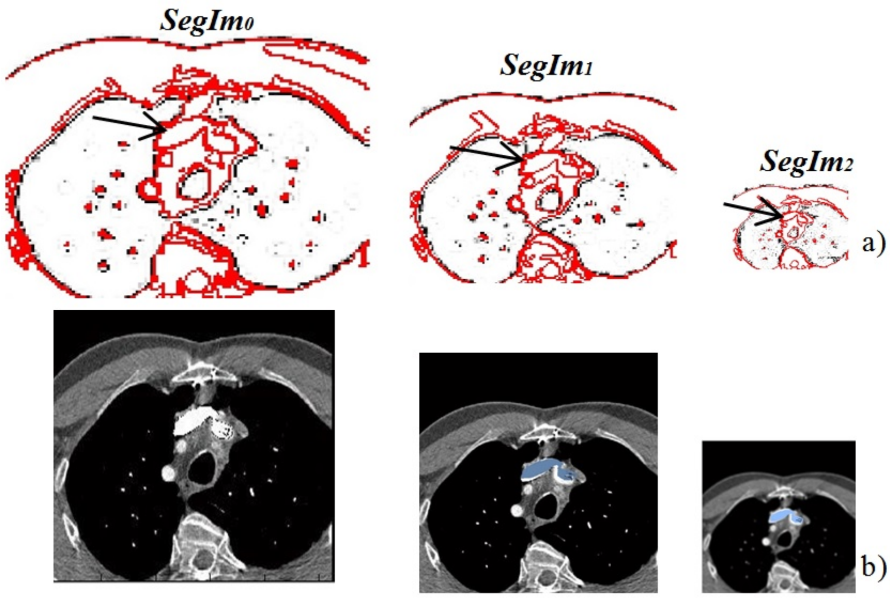

Fig. 6. The result of image segmentation (patient no. 1) a) visualization of the symmetry of the entire anatomical structure, b) the isolated structure of the aorta, at each decomposition level.

When determining the Dice coefficient, the similarity was compared between the structure in original images and in segmented images found at subsequent levels of the pyramid. The average value of the Dice coefficient, obtained during the preliminary statistical analysis, amounted to 0.85. This value was compared with the results in paper [10], whose authors also dealt with medical image segmentation. The average value of the Dice coefficient is close to values obtained by the authors in [10], which proves that the matching level is satisfactory. Hence, the pyramid reduction method may be used as a preliminary stage of medical image processing.

4. CONCLUSIONS

Owing to the application of the pyramid reduction method in the segmentation process, images at various levels of detail are obtained. Images depicting the same structure with different cross-sections make a homogeneous mosaic after being merged. The merging of images featuring the same structure, but in different sharpness planes results in one sharp image. The analysis of images in various scales and planes leads to a precise contour of the structure, without pixel overflow. The contour may be a source of information for the experts during the naked-eye analysis of a specific region or pathological structure. The obtained results during segmentation with algorithms involving the pyramid reduction method are correct, which is proved by the average value of the Dice coefficient amounting to 0.85. In their further research, the authors intend to modify the segmentation algorithms involving the pyramid reduction methods in order to obtain the Dice coefficient at the highest possible level.

BIBLIOGRAPHY

[1] ADELSON E. H., ANDERSON C. H., BERGEN J. R., BURT P. J., OGDEN J. M. 1984, Pyramid methods in image processing. RCA Engineer, 1984, Vol. 29. pp. 33–41.

[2] AVILA-MONTES O., KUKURE U., KAKADIARIS I. A. Aorta segmentation in non-contrast cardiac ct images using an entropy-based cost function. Proc.SPIE, 2010, Vol. 7623. pp. 7623 – 7623 – 8.

[3] BURT P., ADELSON E. The laplacian pyramid as a compact image code. IEEE Transactions on Communications, Apr 1983, Vol. 31. pp. 532–540.

[4] CHOUDHARY B. K., SINHA N. K., SHANKER P. Pyramid method in image processing. Journal of Information Systems and Communication, 2012, Vol. 3. Bioinfo Publications, pp. 269–273.

[5] KOS A., SKALSKI A. Z. T. A modified asm algorithm, that considers a ct and mri medical data anisotropy at the stage of statisticshape model generation. Przeglad elektrotechniczny, 2015, Vol. 5.

[6] LAZEBNIK S., SCHMID C., PONCE J. Beyond bags of features: Spatial pyramid matching for recognizing natural scene categories. 2006 IEEE Computer Society Conference on Computer Vision and Pattern Recognition (CVPR'06), 2006, Vol. 2. pp. 2169–2178.

[7] MOMOT A., WRÓBEL J., HOROBA K., JEŻEWSKI M., BERNYS M. Filtering of two-dimensional digital images using weighted averaging for adaptive selection of weights. Journal of Medical Informatics & Technologies, 2012, Vol. 20. pp. 93–99.

[8] NOAH LEE, HUSEYIN TEK A. F. L. True-false lumen segmentation of aortic dissection using multi-scale wavelet analysis and generative-discriminative model matching. Proc.SPIE, 2008, Vol. 6915. pp. 6915 – 6915 – 11.

[9] PIEKAR E., MOMOT A. Gradient and polynomial approximation methods for medical image segmentation.

[10] SHATTUCK D. W., LEAHY R. M. Brainsuite: an automated cortical surface identification tool. Medical image analysis, 2002, Vol. 6. Elsevier, pp. 129–142.

[11] SKURSKI A., BORZĘCKI M., BALCERZAK B., KAMIŃSKI M., NAPIERALSKI A., KASPRZAK J., LIPIEC P. Image processing methods for diagnostic and simulation applications in cardiology. International Journal of Microelectronics and Computer Science, 2012, Vol. 3. pp. 146–151.

[12] SOBOTNICKA E., SOBOTNICKI A., HOROBA K., PORWIK P. The application of the region growing method to the determination of arterial changes. Computational Collective Intelligence: 8th International Conference, ICCCI 2016, Halkidiki, Greece, September 28-30, 2016. Proceedings, Part II, 2016. Springer International Publishing, Cham, pp. 462–471.

[13] SOBOTNICKA E., WRÓBEL J., SOBOTNICKI A. Detection of aorta anatomical structures characterized by various levels of pixel intensity. 2016 MIXDES - 23rd International Conference Mixed Design of Integrated Circuits and Systems, June 2016. pp. 498–503.